Proceedings of the 2024 14th International Pipeline Conference
IPC2024
September 23-27, 2024, Calgary, Alberta, Canada

IPC2024- 133317

IN-SITU DETERMINATION OF PIPE BODY FRACTURE TOUGHNESS USING PLANING-INDUCED MICROFRACTURE METHOD

Xuejun Huang
Massachusetts
Materials Technologies
Natick, MA

Bryan Feigel
Massachusetts
Materials Technologies
Natick, MA

Aidan Ryan
Massachusetts
Materials Technologies
Natick, MA

Intisar Rizwan I Haque
Massachusetts
Materials Technologies
Natick, MA

Brendon Willey
Massachusetts
Materials Technologies
Natick, MA

Simon C. Bellemare
Massachusetts
Materials Technologies
Natick, MA

ABSTRACT

Pipe toughness determination as part of nondestructive evaluation (NDE) has been sought for decades. Material toughness is needed when analyzing the critical crack size that would fail at MAOP and when performing a fitness-for-service evaluation with cracks discovered during an inspection. When toughness data is not available, operators may use conservative values, perform cut-outs for lab testing, or use other industry-accepted data, such as collected by nondestructive testing. This paper presents a new in-situ, minimally invasive technique to provide pipe body toughness data using the method of planing-induced microfracture. This method involves using a specialized blade featuring a central opening where the material is stretched and fractured instead of being cut, leading to standing residual ligaments on the fractured surfaces of the sample. Characteristics of these ligaments, such as their height, are shown to correlate with the material's fracture toughness. Preliminary proof-of-concept testing from 30 samples showed that the method could predict K_{Ic} *to within ±20% of the values derived from destructive lab testing [1]. In the work presented in this paper, a portable prototype instrument has been developed which can create "islands" on a pipe surface and perform the planing-induced microfracture test. This paper will give an overview of the planing-induced microfracture method, the prototype field instrument, and recent test results using the tool.*

Keywords: nondestructive, fracture toughness, planing-induced microfracture

NOMENCLATURE

BTM	blade toughness meter
CTOD	crack tip opening displacement
CVN	Charpy V-notch
LH	ligament height
MAOP	maximum allowable operating pressure
NDE	nondestructive evaluation
NDTT	nondestructive toughness tester
SH	stretch height
K_{Ic}	fracture toughness
K_f	toughness (area under the stress-strain curve)
σ_y	yield strength
σ_u	tensile strength
ε_f	elongation at break

1. INTRODUCTION

Fracture toughness can be defined as the critical value of the stress intensity factor for which a crack propagates. While performing a fitness-for-service analysis for a cracked component, fracture toughness serves as a key input for the analysis and determines whether the crack, as it is now or in the future, is safely tolerated within the design limits of the components. However, for many vintage pipelines, records of fracture toughness are not available as they were not required in the earlier versions of the API 5L specifications for line pipe. Conventional testing methods for fracture toughness include testing using compact or single-edge bend specimens. An alternative is the Charpy impact test which is an indirect method that provides an energy value that can be used to estimate the toughness of materials using empirical correlations. These methods are destructive and require cut-out samples from pipes, which are not always desired or cost-effective.

Over the past decade, several NDE solutions have been developed to help determine pipe toughness. In PRCI project

NDE 4-C, BMT Fleet Technology [2] developed a neural network model that uses pipe hardness, chemistry, and microstructure information to predict the CVN impact energy values at five selected temperatures ranging from -20 to 40 ˚C. Data from 118 vintage (pre-1970's) pipe samples were collected and used to train and validate the model. The model in general showed an accuracy of within ±10 J (or 7.4 ft-lbs.) compared to lab values. Future work was noted in this study including a blind test to further evaluate the accuracy of the model. Similarly, Switzner et al. [3] developed random forest models using different combinations of chemical elements and microstructure inputs (grain size and dark phase percentage) to predict CVN upper shelf energy and transition temperature. Their results indicated that sulfur, silicon, carbon, and manganese as well as the dark phase percentage are the strongest predictors for those values.

Lee et al. [4] proposed a model to predict fracture toughness using the instrumented indentation technique (IIT). The authors introduced the concept of critical indentation depth, which can be determined by measuring and extrapolating the relationship between indentation depth and degraded elastic modulus. While the authors claimed that there was a similarity in stress triaxiality ahead of a spherical indenter in their testing and ahead of the crack tip in a CTOD test, they failed to explain why cracking was not observed in their indentation tests and thus the critical indentation depth can only be obtained through extrapolation of the experimental data. Haggag developed the automatic ball indentation (ABI) technique utilizing a similar concept of critical indentation depth and successfully predicted the fracture toughness for high toughness steels (>180 ksi√in) [5].

Palkovic et al. [6] developed a nondestructive toughness tester (NDTT) to measure fracture toughness using a specially designed wedge-shaped stylus with a central opening called a stretch passage to generate a tensile fracture on the surface of a specimen. It was shown that a ductile fracture was successfully generated within the opening as the blade cut across the specimen surface and the height of residual ligament on the substrate and chip surfaces correlated to the material fracture toughness. The results of that study correlated better with CVN values than with fracture toughness values.

The NDTT design used in the study by Palkovic et al. [6] has been improved in 2022 [1]. The new design adopted the earlier stretch passage concept, but the wedge with a total included angle of 65º was replaced by a sharper blade with a total included angle of 25º. This provides the benefits of less shear plastic deformation of the material ahead of the blade and a higher state of material stress triaxiality within the stretch passage. The change in concept to decrease the included angle by a factor of more than two is in the new requirement that both the top and bottom sides of the blade are engaged with the test sample such that the reaction forces counteract and prevent excessive bending stresses in the blade.

2. MATERIALS AND METHODS

2.1 Method of Planing-Induced Microfracture

The testing method of the current study was termed "Planing-Induced Microfracture" [1]. The key underlying concept of this method is to introduce a near-surface microcrack from which features can be extracted and correlated to the material fracture toughness. It uses a specialized blade with a central opening to plane the surface of a specimen. As the blade moves across the surface, the material at the central opening is uncut and flows through the opening while it is subjected to tensile stress until it fractures (Figure 1). This opening is referred to as the "stretch passage," as the material passing through it experiences primarily tensile strain. When the material fractures, residual ligaments remain on the fractured surface of the substrate and the opposite face of the separated chip. The characteristics of these ligaments, such as their height and the crack front profile within the stretch passage, correlate with the material's fracture toughness, as discussed later in this paper.

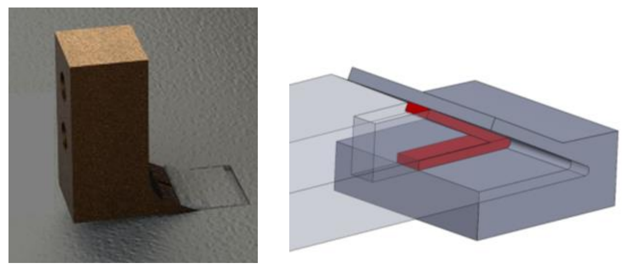

FIGURE 1: PLANING-INDUCED MICROFRACTURE METHOD

Figure 2 shows the cross-section of a sample within the stretch passage, taken by grinding the side of the sample. This figure shows that a crack has been formed and propagated within the strength passage along with the movement of the blade. The zig-zag character of the crack reveals the effect of grain orientation. An example of a top view of the ligament within the stretch passage revealing the ductile fracture feature can be found in [6].

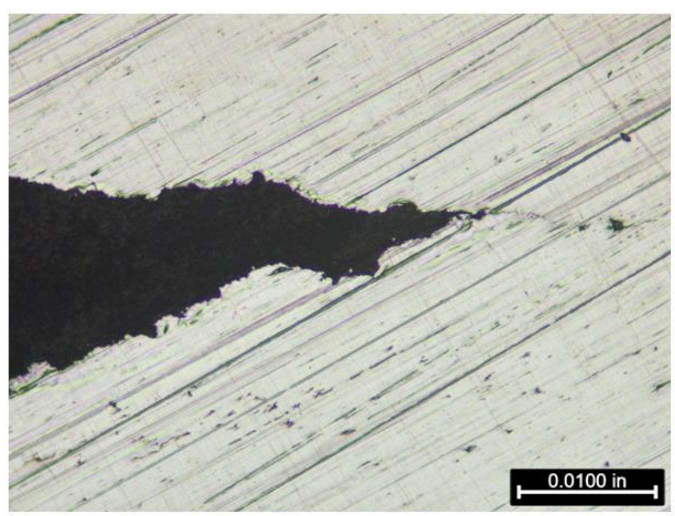

FIGURE 2: CROSS SECTION OF CRACK TIP WITHIN THE STRETCH PASSAGE

2.2 Surface Testing Implementation

A field tool for measuring pipe body fracture toughness, called Blade Toughness Meter (BTM), was built by Massachusetts Materials Technologies (MMT) implementing the planing-induced microfracture method. This paper presents the first validation test of the tool, the data processing procedure, and the preliminary results. The experimental data presented below was collected on cut-out oil and gas pipeline sections at an MMT customer facility and at MMT.

Pipes were staged on pipe stands whereafter the BTM tester was secured onto them. The securing system consists of pipe attachment "feet" integral to the BTM tester frame and ratchet straps. These aluminum feet straddle the circumference of the pipe and are brought into rigid contact with the pipe by tightening of the ratchet straps (Figure 3). The securing system is designed to work on pipes with outer diameters ranging from 8 to 48 inches.

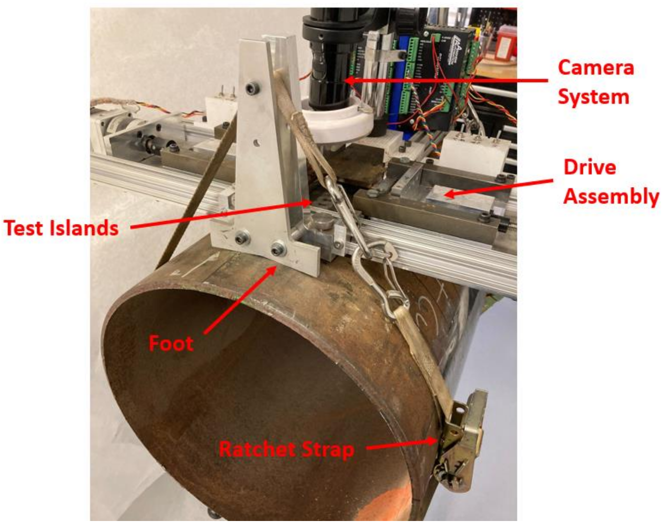

FIGURE 3: BTM TEST SETUP.

Testing of a pipe begins by preparing raised 'islands' of material which are then 'planed' off during the microfracture test. The 'islands' are formed using a custom 1-inch non-plunging end-mill bit and a Euroboor ECO.36+/T magnetic drill (mag drill). The mag drill is placed into the BTM tester, wherein features of the tester assist an operator in adequately orienting the drill to the pipe, positioning it for drilling, and rigidly securing it to avoid mishandling or drill chatter. The non-plunging end-mill bit ensures material removal at the edges of the bit but no deeper than 0.030-inch depth due to a central flat recessed limit stop within the bit. As a result, the mag drilling will leave behind a raised circle of material up to – but not exceeding 0.030 inch. The mag drill performs the machining operation at six prescribed locations of which the spacing is such that overlap results in four slightly curved rectangular islands (Figure 4).

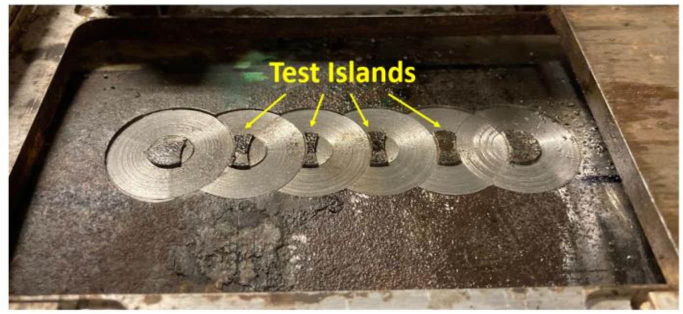

FIGURE 4: MACHINED TEST ISLANDS ON PIPE SURFACE.

Once the islands have been prepared, the microfracture test may proceed. The islands are tested with two tungsten carbide blades driven into the island from opposite sides; one side utilizes a blade with a 0.020-inch stretch passage and the other, a 0.015-inch stretch passage. The orientation is such that the blades are moving along the circumferential direction of the pipe during testing. The blade is brought into contact with the machined surface immediately outside the island and then driven into the island to 'plane' it off the pipe (Figure 5). Examples of the substrate and the formed chip after testing are shown in Figure 6.

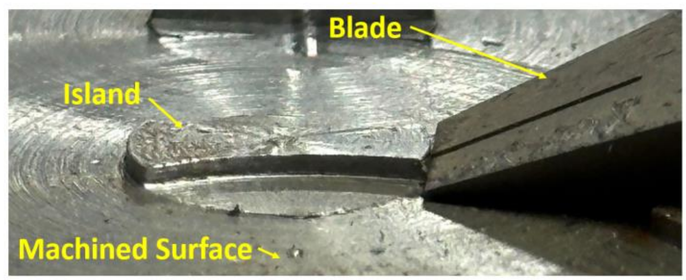

FIGURE 5: BLADE PLANING OFF TEST ISLAND (ONLY SHOWING ONE OF TWO BLADES).

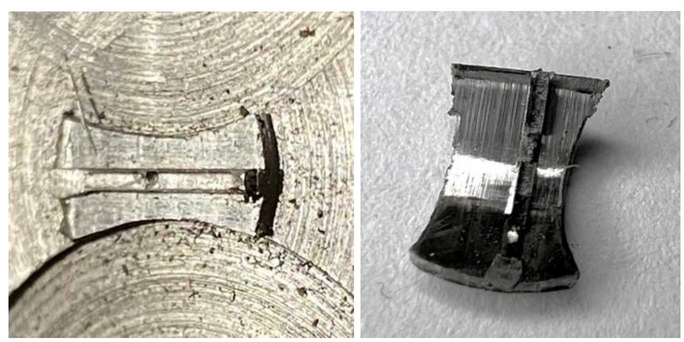

FIGURE 6: SUBSTRATE (LEFT) AND CHIP (RIGHT) AFTER TESTING.

After each blade has traveled approximately 0.017 inch, the test is stopped to initiate crack front characterization measurements (described in detail in section 2.3) which includes dying the ligament with a surface dye via administration with a syringe, and taking images with a microscope to capture the blade position with respect to the crack front. After these measurements are taken, the test is restarted and finishes once the two blades have cut through nearly the entire island and the chip is removed. Upon removal of the chip, the final images of the ligament and dyed crack front are taken with the microscope and the ligament on the chip and pipe substrate are scanned with a laser scanner.

2.3 Crack Front Characterization

As mentioned in Section 2.2, analysis of the crack front produced by each blade serves as a key input to the prediction of fracture toughness. Crack front characterization includes an analysis of the crack shape and a measurement of the blade position with respect to the crack front when the crack was formed. This distance between the crack front and the blade position is called the 'lag'.

During a BTM test, the blade is stopped after a steady-state material response is achieved, which takes approximately 0.17 inch, as shown through historic testing. Once the test is paused a syringe containing a surface dye is inserted into the stretch passage to dye the entire ligament up to the crack, including the crack tip. The surface dye is allowed to sit for approximately 3 minutes, after which the dye is neutralized with an aqueous solution and cleaned with compressed air. The blade position is imaged with a microscope and camera to be later compared to the location of the exposed crack front.

After surface dying, the test is continued until the opposing blades nearly meet and the chip can be removed. Once the chip is removed, an image is taken, in the identical position as the blade position image taken previously, showing the exposed, dyed, crack front and ligament. The two images, one of the blade position, and the second of the exposed crack front, are superimposed to allow for the measurement of the blade position with respect to the crack front (lag measurement). Figure 7 shows an image of the exposed and dyed crack fronts after testing a single island with a blue line on the left representing the original blade position and shows a zoomed-in image of the crack front.

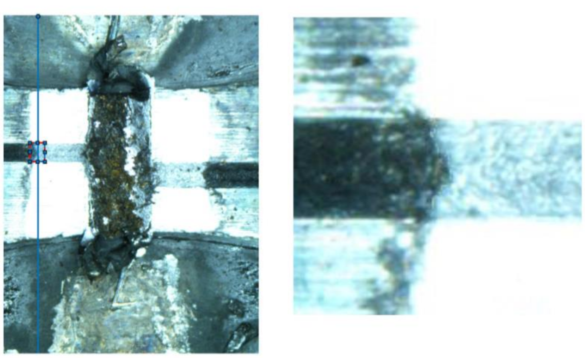

FIGURE 7: PIPE SUBSTRATE AND EXPOSED, DYED, CRACK FRONTS (LEFT) AND ZOOMED-IN CRACK FRONT (RIGHT)

Once the crack front and the blade positions are identified, the lag is measured between the crack front position in the center region and the blade edge position (Figure 8).

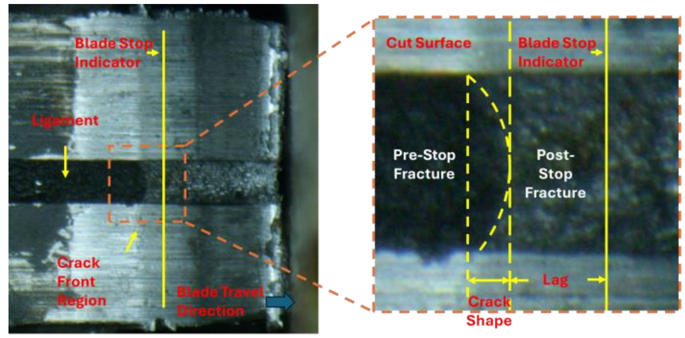

FIGURE 8: CRACK FRONT PROCESSING AND LAG MEASUREMENT

2.4 Ligament Height Characterization

Upon completion of a BTM test, the ligament on the pipe substrate and chip are scanned with a laser scanner to extract geometric features, including the average ligament height. Custom software was developed to process the scanned ligament data (Figure 9). The process begins by cropping the pipe and chip scans to isolate the ligament feature and the cut surface of the island. A user then defines the cut surface on either side of the ligament by selecting it on a 3D-rendered plot of the cropped scan. To calculate the height for each cross-section scan of the ligament, the software measures the average height of the ligament region relative to the cut surface. Two defined regions were compared for height calculations during this study. The 'Zone' calculation returns the average height across the entirety of the ligament, and the 'Third' calculation returns the average height across the center third of the ligament.

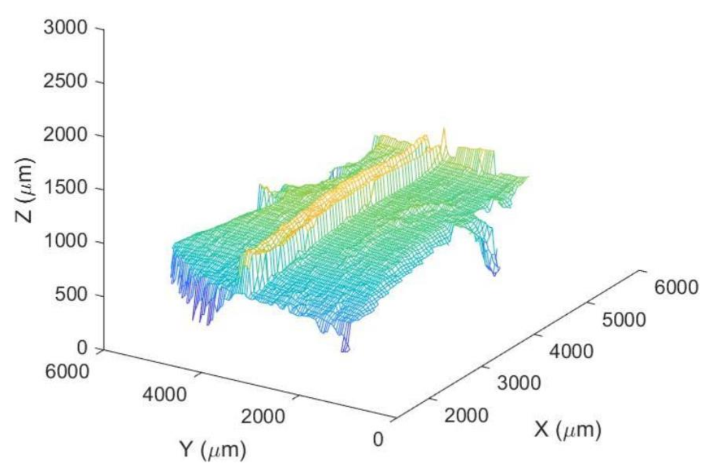

FIGURE 9: 3D LASER SCAN OF PIPE SUBSTRATE LIGAMENT

After calculating the pipe and chip scan ligament heights, the Ligament Height vs. Test Distance plots are aligned via the initial region of the tests (Figure 10). Subsequently, the chip scan is 'stretched' using a linear scaling factor to account for the curvature of the chip. After alignment, the two ligament height profiles are aggregated to achieve a smooth total ligament height profile. The initial region of the test is typically of an increased height corresponding to the initial tensile response leading up to the generation of the fracture. After the fracture begins to propagate, the height of the ligament stabilizes and reaches a region (Figure 10, highlighted in yellow) referred to as the 'steady-state region'. The average ligament height in the steady-state region is calculated and used in the later analysis.

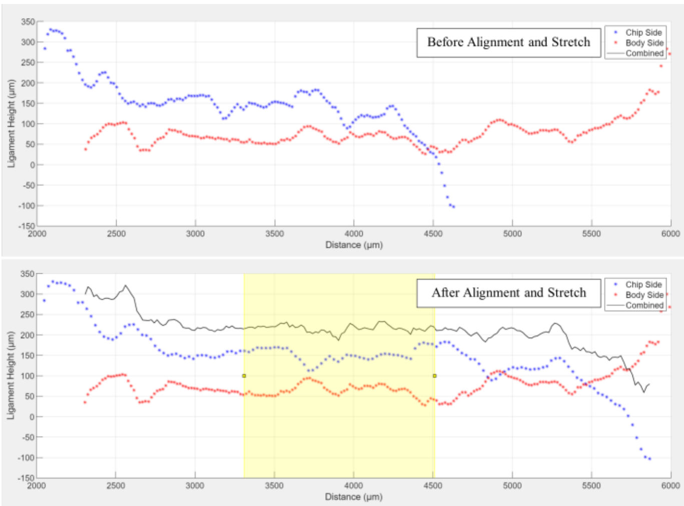

FIGURE 10: AVERAGE LIGAMENT HEIGHT VS TEST DISTANCE PLOTS FOR THE SUBSTRATE, CHIP, AND COMBINED LIGAMENT WITH THE STEADY STATE REGION HIGHLIGHTED IN YELLOW

3. RESULTS

A total of 18 pipe cutouts were tested using the BTM field protype instrument. Lag and ligament height data were processed as described in Section 2.3 and Section 2.4. At least two quadrants are tested for each pipe cutout. For ligament height, test results are averaged for each quadrant, and the smallest value of all quadrants was used for that sample. For lag measurement, due to the limited number of high-quality images, the smallest value of all available tests was used for each sample. After reviewing the fitting results using the physical model described below, the ligament height data using the 0.015-inch stretch passage gives a better result than the 0.020-inch stretch passage and thus is used in the following analysis.

Destructive lab testing was performed to obtain the yield, tensile and fracture toughness data per ASTM A370 and E1820 using third-party labs. For fracture toughness testing, each pipe was tested three times, and the minimum value was reported as final value by the labs per industry standard. These lab data are used to calibrate the prediction model described later in this section.

Upon reviewing the variation of the BTM and lab testing data, a criterion of maximum 15% of standard deviation is applied which filters out four samples, two due to variation in ligament height measurement, and two due to variation in lab-tested fracture toughness. A total of 14 samples were used in the analysis.

The built prediction model was previously introduced in [1]. According to Oh [7], the fracture toughness (K_{Ic}) and the toughness measured using the area under the tensile stress-strain curve up to the elongation at break (K_f) are correlated:

$$\left(K_{Ic}/\sigma_y\right)^2 = \alpha \left(K_f/\sigma_y\right)^2 \tag{1}$$

where σ_y is the material's yield stress and α is a constant for a certain group of material (e.g. carbon steels). The area under the stress-strain curve can be estimated using the yield strength, ultimate tensile strength (σ_u), and elongation at break (ε_f) [5]:

$$K_f \approx \varepsilon_f \left[k\sigma_y + (1-k)\sigma_u\right] \tag{2}$$

where k is a weighted coefficient to account for the nonlinearity of the stress-strain curve and $0 < k < 1$.

In the previous publication [1], a hypothesis was proposed that the measured ligament height (LH) is linearly proportional to the elongation at break considering the material within the stretch passage is subjected to predominantly tensile stress and stretched to failure:

$$\varepsilon_f = a * LH + b \tag{3}$$

where a and b are fitted coefficients. In this paper, an adjusted version of Equation (3) is also evaluated, where the ligament height is replaced by the stretch height (SH) which can be expressed using the lag measurement (Figure 11):

$$SH \approx Lag * \tan(25°) \tag{4}$$

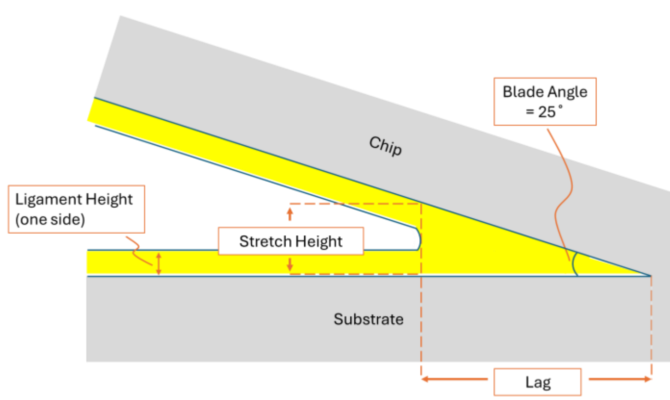

FIGURE 11: SCHEMATIC OF THE STRETCH HEIGHT

Combining the equations above and with some modifications, we have the following correlation between K_{Ic} and stretch height:

$$K_{Ic}/\sigma_y = C_1 * \left[k + (1-k)\sigma_u/\sigma_y\right] * SH + C_2/\sigma_y + C_3 \quad (5)$$

where C_1, C_2, C_3 and k are fitted coefficients using the data of the 14 test samples.

A machine learning (ML) model was developed using the predicted K from the physical model, tensile strength, and selected chemical composition to further improve the prediction accuracy. Nine samples were used to train the ML model, and the remaining five samples were used to validate the ML model. Only three features were used as model inputs to ensure that the ML model did not overfit the available data. The performance of the different models is compared in Table 1. The machine learning model using ligament height yields the best performance. Figure 12 shows the predicted K values using this model vs. lab-tested values. For most data points (12 out of 14), the predicted values are within ±20% of the lab-tested values. In relationship to the prior study with a non-portable lab instrument [1], the new test configuration with the instrument attached to pipe cylinders did not alter the measurement accuracy.

TABLE 1: PERFORMANCE OF DIFFERENT MODELS

Model	Root Mean Square Error (RMSE)	R2 Score
Physical Model using Ligament Height	21.9	0.68
Machine Learning with Ligament Height (Selected)	11.8	0.91
Physical Model using Stretch Height	20.37	0.73
Machine Learning with Stretch Height	15.3	0.84

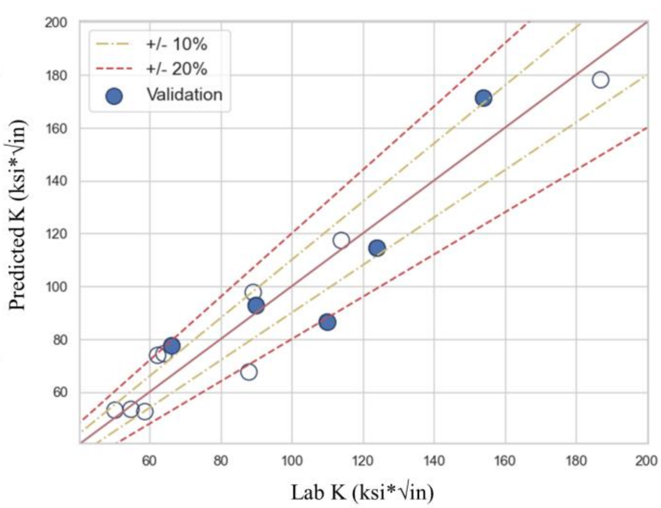

FIGURE 12: UNITY PLOT OF PREDICTED K VALUES VS. LAB TESTED K VALUES (EMPTY CIRCLES ARE TRAINING DATA AND SOLID CIRCLES ARE VALIDATION DATA)

4. DISCUSSION

4.1 BTM Testing Configuration

4.1.1 Crack Direction

The current BTM testing setup introduces a sub-surface microcrack which propagates in the pipe circumferential direction and is oriented with the crack plane normal in the thickness direction. This is different from the crack orientation in a compact tension specimen used in lab fracture toughness testing for pipes. A compact tension specimen usually has a C-L configuration where a through-wall crack grows in the longitudinal direction and the crack plane normal is in the circumferential direction. Note that it would not be practical to introduce a through-wall crack to a live pipeline. Considering the texture of pipeline steels resulting from their manufacturing processes, the material response from BTM testing might be different from lab testing.

However, a correlation to lab-tested fracture toughness is still possible as shown in Section 3 and previous study [1]. The issue may be further addressed through feeding relevant information (pipe wall thickness, pipe diameter, grain size, etc.) to the machine learning models to account for the different crack orientations.

4.1.2 Cut Depth

The targeted cutting depth for the mag drill is 0.030”. Note that for surface testing such as hardness testing, API 579 recommends the removal of about 0.020 inch of material from surface to avoid oxide scale and surface decarburization. Therefore, the current cutting depth is believed to be sufficient to avoid these surface anomalies and reveal the true material response. No surface removal or polishing is needed for the BTM testing.

4.2 Applicability of BTM Testing

When pipe body toughness data is not available, the current US regulation (49 CFR § 192.712) allows the use of a conservative value of 13.0 ft.-lbs for pipes with no history of reportable incidents, or for the operator to perform cut-outs for lab testing to derive values. Using the default value from CFR, assuming a yield stress of 45 ksi and using the Rollfe-Novak-Barsom correlation [8] following API 579, the corresponding fracture toughness is approximately 50 ksi*√in (This value changes to 44 ksi*√in for 35 ksi yield and 53 ksi*√in for 55 ksi yield).

MMT has access to 60 pipe samples that have been lab-tested for fracture toughness at 32 °F. The distribution of fracture toughness for these samples is shown in Figure 13. By fitting a normal distribution to these data, it is shown that 96% of the samples in our database have fracture toughness values above the regulation default of 50 ksi*√in. In addition, 80% of the fracture toughness values are above 75 ksi*√in and 46% are above 100 ksi*√in. This suggests that performing the BTM testing could potentially help operators obtain higher and more accurate toughness values for their pipelines, which ultimately avoids unnecessary repair of cracks.

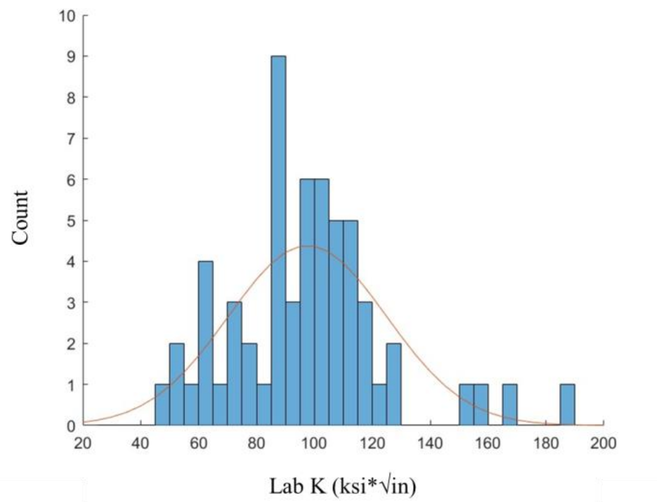

FIGURE 13: HISTOGRAM OF FRACTURE TOUGHNESS DISTRIBUTION OF MMT SAMPLES

4.3 Future Development

There are multiple directions being considered to further improve the accuracy of the BTM instrument.

Performing more tests to collect more data will help further improve the performance of the physical model and machine learning model. MMT plans to conduct a Joint Industry Program (JIP) and aims to add 200+ samples to our database. More data also allows the machine learning model to use additional input such as grain size and more chemical compositions, which may improve the model's accuracy.

Furthermore, since the planing-induced microfracture method introduces a true crack into the sample, fracture surfaces can be imaged directly from the substrate or the chip, which may be utilized to assess fracture properties [9].

5. CONCLUSION

A field prototype implementing the planing-induced microfracture method has been evaluated for readiness by testing pipe cylinders removed from service. Physical and machine learning models were built to correlate the ligament height and the crack front lag measurement to the material fracture toughness. Preliminary results show that most predicted fracture toughness values fall within ±20% of the lab-tested values. This level of accuracy is similar to what was previously obtained using a laboratory prototype where small samples were cut and attached to a fixed instrument, thereby successfully demonstrating the field prototype design.

These results will be leveraged to help further refine the prototype tool design and the test procedure. More test data will be collected to improve the current prediction models for better accuracy.

REFERENCES

[1] Huang, Xuejun, et al., Validation of Planing-Induced Microfracture for Determining Pipe Body Toughness, Pipeline Pigging and Integrity Management (PPIM) (2024).

[2] Amend, B., S. Riccardella, and A. Dinovitzer. Material verification–validation of in situ methods for material property determination, PRCI NDE-4-8, 2018.

[3] Switzner, N., et al., Assessing steel pipe toughness using chemical composition and microstructure, Pipeline Pigging and Integrity Management (PPIM) (2021).

[4] Lee, Jung-Suk, et al. An instrumented indentation technique for estimating fracture toughness of ductile materials: A critical indentation energy model based on continuum damage mechanics, Acta Materialia 54.4 (2006): 1101-1109.

[5] Haggag, Fahmy M. "In-Situ Measurement of Pipeline Mechanical Properties Using Stress-Strain Microprobe—Validation of Data for Increased Confidence & Accuracy." PRCI Report L52280 (2007).

[6] Palkovic, Steven D., et al., Calibration of a nondestructive toughness tester (NDTT) for measuring fracture toughness of pipeline steel, International Pipeline Conference. Vol. 51869. American Society of Mechanical Engineers, 2018.

[7] Oh, Gyoko, A simplified toughness estimation method based on standard tensile data, International Journal of Pressure Vessels and Piping 199 (2022): 104733.

[8] Barsom, J.M. and Rolfe, S.T., Fracture and Fatigue Control in Structures, Third Edition, Prentice Hall, Englewood Cliffs, New Jersey, 1999.

[9] Dey, Surajit, Ravi Kiran, and Chad Ulven. Experimental Evaluation of Microvoid Characteristics and Relationship with Stress and Strain for Ductile Fracture. Journal of Materials in Civil Engineering 36.2 (2024): 04023573.